International Journal of Modern Physics C
Vol. 30, No. 11 (2019) 1950099 (12 pages)

DOI: 10.1142/S0129183119500992

Modeling an HPGe detector response to gamma-rays using MCNP5 code

I. V. Prozorova

Institute of Atomic Energy
National Nuclear Center of the Republic of Kazakhstan
P.O. Box 071100, Kurchatov, Kazakhstan
prozorova@nnc.kz

R. R. Sabitova

School of Nuclear Science and Engineering
Tomsk Polytechnic University
P.O. Box 634050, Tomsk, Russia
radmila1@tpu.ru

N. Ghal-Eh*

School of Physics
Damghan University
P.O. Box 36716-41167, Damghan, Iran

Department of Physics
Faculty of Sciences
Ferdowsi University of Mashhad
P.O. Box 91775-1436, Mashhad, Iran
ghal-eh@du.ac.ir

S. V. Bedenko

School of Nuclear Science and Engineering
Tomsk Polytechnic University
P.O. Box 634050, Tomsk, Russia
bedenko@tpu.ru

Received 28 January 2019
Revised 29 July 2019
Accepted 31 August 2019
Published 30 September 2019

The response function is the important information for the precise interpretation of experimental data and also for characterizing the developing nuclear instruments. Measurement of the response function normally requires a number of mono-energetic gamma-ray sources, a long acquisition time and an appropriate experimental setup. The Monte Carlo method, as an alternative to response function measurement, has widely been used and recommended. In this study, a computational model of an HPGe detector has been developed by using the MCNP5

*Corresponding author.

code. To validate the simulated model, the simulations from mono-energetic sources have been compared to the corresponding measured data. Any deviation from the measurement could be attributed to the unmodeled details of the detector crystal, so they needed adjustment. Moreover, an analysis has been undertaken on the dependency of detection efficiency on the dead layer thickness of the germanium crystal. Having developed a computational model of the crystal, a set of correction factors was extracted to take into account the gamma-ray self-absorption within the source volume. The simulated model of the HPGe detector in this study can be used to calculate the detection efficiency when the samples are not of the standard geometry which require self-absorption considerations.

Keywords: HPGe; MCNP5; dead layer; gamma-ray.

PACS Nos.: 28.52.Av, 29.40.Wk.

1. Introduction

The semiconductor detectors are widely used in radiation measurement. They have a leading place among different radiation detection devices due to a number of advantages, such as excellent energy resolution, linearity over a wide range of energies, short pulse rise-time, simplicity, very small dimensions and the insensitivity to magnetic fields.[1–4]

Research studies have been undertaken on different aspects of HPGe detectors, including the new technologies for producing semiconductor detectors, methods for calibrating and measuring geometric parameters and so on.[5–9] High-resolution spectroscopy of penetrating charged particles is an interesting topic which requires us to know the thickness of insensitive region (i.e. the dead layer) of the HPGe to obtain the incident particle energy. The incident particle energy is determined by taking a summation over both the deposition energy inside the detector and the average energy loss in the dead layers. Therefore, the thickness of both the sensitive and dead layer is necessary to take into account for particle identification and spectroscopy through the registration of the events in which the energy changes occur due to nuclear interactions. The most accurate approach to the measurement of sensitive and dead layers of HPGe detector is the use of accelerated beam. However, this approach has limited application because of the long-term measurement with accelerators.

In an undertaken study,[9] the dead layer measurements of a standard HPGe detector were carried out with a ^{207}Bi source. The 975 keV internal conversion electrons of ^{207}Bi were incident on the HPGe whose range was dependent upon the source thickness. The dead layer of HPGe was so determined that for each detector a calibration dependence was constructed. Then, the detector under study was turned so that the dead layer (i.e. p^+-contact) was faced to the source. The shift of the internal conversion electron peak could determine the dead layer thickness.

In this work, the dead layer thickness of a semiconductor detector made of high-purity germanium was measured by the fact that gamma-ray detection efficiency of HPGe depends on the parameters of the dead layer; therefore, the dead layer thickness can be determined through detector modeling. The detector simulation and

response function calculation were carried out with the general-purpose Monte Carlo N-particle code, MCNP5.[5,6,8–11]

2. Materials and Methods

2.1. *Simulation of a Canberra GC1518 HPGe detector*

The semiconductor coaxial HPGe detector, type GC1518, has a relative detection efficiency of 15%, the energy resolution of 1.8 keV at 1332 keV line, a good peak shape and a low level of leakage currents (about 10^{-11} A). The detector is a cylindrical high-purity germanium detector (Fig. 1) with a large volume of a sensitive region (from 20 to 100 cm^3). The n-electrode is a lithium layer (0.6 mm thick) on the outer surface of the cylinder, while the implanted boron layer (0.3 μm thick) on the inner surface of the central hole serves as a p-electrode.[12]

The geometry and material definition of the detector have been provided by the official supplier of Canberra gamma spectrometers; however, the arrangement of the electrodes was not clearly determined. If the electrodes thickness is considered in the linear dimensions of the crystal, the sensitive volume of the detector decreases which itself alters the detector response. Since the contact thickness with boron layer is insignificant, the lithium contact has the main contribution to the crystal volume from the electrodes sides.

Two different detector models have been constructed: in Model 1, the crystal volume has included the thickness of the lithium contact, while in Model 2, the contact thickness is not included in the dimensions of the crystal. Figure 2 shows a

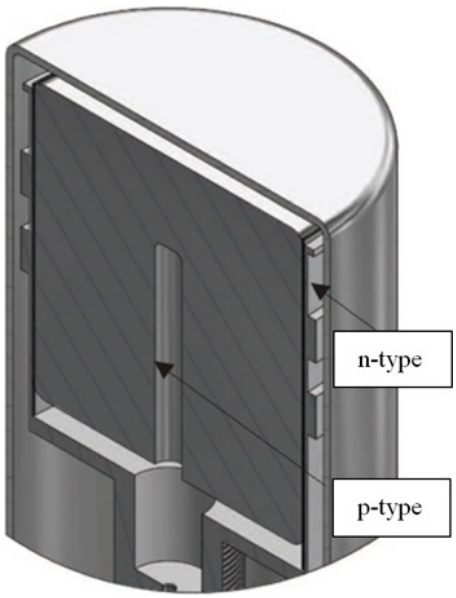

Fig. 1. The sketch of a cylindrical germanium detector.

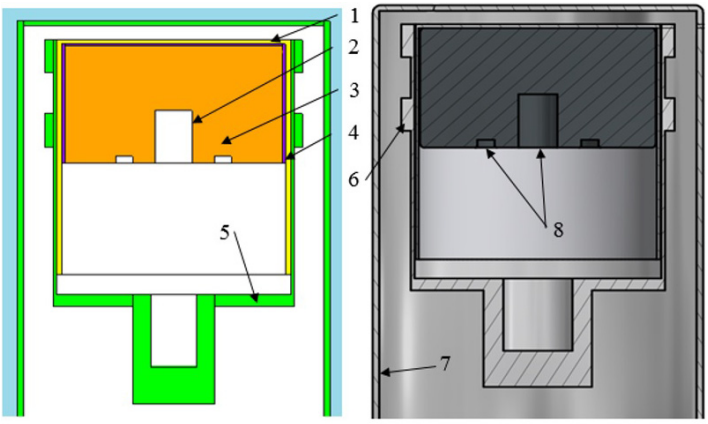

(a) (b)

Fig. 2. (Color online) (a) MCNP-built model and (b) manufacturer sketch of Canberra GC1518 germanium de-tector: (1) High-density polyethylene; (2) Boron contact layer; (3) Germanium crystal; (4) Lithium contact layer; (5) Aluminum holder; (6) O-rings; (7) Aluminum cryostat; (8) Hole.

comparison made between the germanium detector modeled with the MCNP5 and the original manufacturers sketch.

2.2. *Modeling detector response and the dead layer thickness determination*

A germanium detector together with a ^{152}Eu gamma-ray source located at a distance of 80 mm has been selected for the simulation. In order to compare the detector response with the available measured data (experimental results were obtained in 2016 at the Institute of Atomic Energy of the Republic of Kazakhstan inside the framework of the program to substantiate the neutron-physical characteristics of the conversion core of the IVG.1M reactor, protocol No. 13-240-02/1078 of July 01, 2016), it is necessary to consider a series of gamma-ray energies and carry out the detection efficiency calculations for two different detector models. The calculations have been performed for 2.5E7 primaries to make sure that the relative errors of the MCNP calculations remains below 1.0%. The relative deviation, R, has been also calculated for the gamma-ray energies listed in Table 1.

Since the comparison shows that the detection efficiency values calculated with Model 1 has less deviation than the corresponding measured ones, the remaining calculations have been carried out with this model.

The majority of deviations from the measured values are due to the fact that both models have been constructed without taking into account the dead layer. The dead layer is basically defined as the region between the outer surface and the sensitive volume of the detector wherein the interaction of ionizing radiation generates no signal. The produced particle charge within the dead layer is not fully collected due to such reasons as, its lower resistance from the main conductors, the greater number

Table 1. Comparison of calculated and experimental data.

Gamma-ray energy E_γ, keV	Detection efficiency, $\varepsilon \cdot 10^{-3}$ RU			Relative deviation R, %	
	Measured value	MCNP5 value, Model 1	MCNP5 value, Model 2	Model 1	Model 2
121.78	14.1	16.9	17.8	19.6	26.50
244.70	8.18	9.50	10.1	16.2	23.77
344.28	5.69	6.33	6.78	11.3	19.16
443.98	4.24	4.73	5.08	11.5	19.72
778.9	2.33	2.62	2.83	12.5	21.50
867.38	2.04	2.37	2.55	15.9	25.24
964.13	1.88	2.15	2.32	14.3	23.52
1085.9	1.71	1.92	2.09	12.5	22.06
1112.1	1.64	1.89	1.97	15.0	19.82
1407.99	1.30	1.53	1.65	17.8	27.11

of traps associated with the surface treatment of the semiconductor, the deposition of the electrode layer which is usually accompanied by a shorter mean life and the lower electric field strength.[11] The dead layer measurement is important in accurate radiation spectroscopy because it both degrades the energy resolution and reduces the energy determination accuracy, which is dependent on the atomic shells structure.[6,11,13–15]

Next, the effective thickness of the dead layer has been calculated. To this purpose, an additional layer has been added to the crystal geometry model, which was not geometrically different from germanium but could influence the detection efficiency. The accurate dead layer thickness may be calculated by changing the upper and lateral dead layer thicknesses. Then, an assessment is necessary to estimate how dead layer thickness would affect the detection efficiency. The dead layer thicknesses are eventually corrected until the difference between the calculated and the measured responses becomes minimally acceptable despite the experimental errors.

Different calculations have been carried out with a ^{152}Eu gamma-ray source which is located at 80, 100, 150, 200 and 250 mm far from the end surface of the detector housing, similar to the conditions used for the calibration. The variation of detection efficiency against the dead layer thickness is shown in Fig. 3.

The data in Fig. 3 demonstrates that the detection efficiency decreases with increasing dead layer thickness, or equivalently, by decreasing the sensitive volume of the crystal. Finally, using the above detection efficiency values, the correct choices of the top and side dead layer thicknesses for GC1518 crystal have been calculated so that the effective thickness has been set to 0.7 mm for all layers.

2.3. *Comparison with measured values*

Figure 4 shows that for a variety of source-to-detector distances, the calculated detection efficiency values, when plotted against the gamma-ray energy, represent an

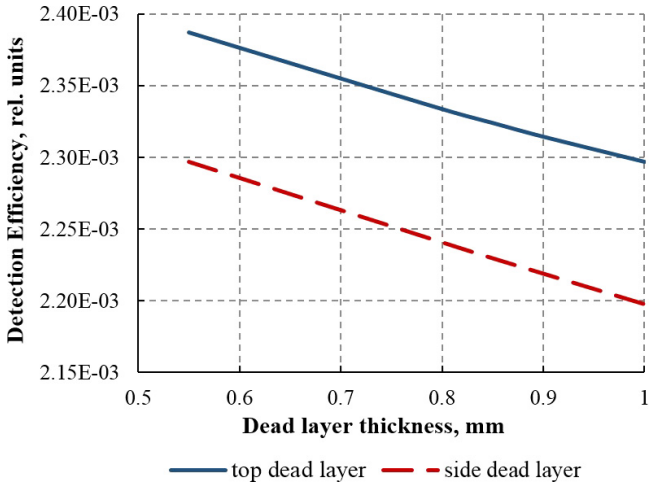

Fig. 3. (Color online) Variation of detection efficiency versus the dead layer thickness.

exponential decay behavior. For short distances, a sudden drop in detection efficiency is observed with increasing gamma-ray energy. As the source-to-detector distance increases, the low-energy gamma-rays interacting with the surrounding materials do not reach the sensitive volume of the detector; hence, they are registered almost as high-energy gamma-rays.

The deviations of the model response from the physical detector is illustrated in Fig. 5 for the smallest, the largest and optimal (100 mm) source-to-detector distances. The measured data have been taken as true values and set as unity for a better comparison.

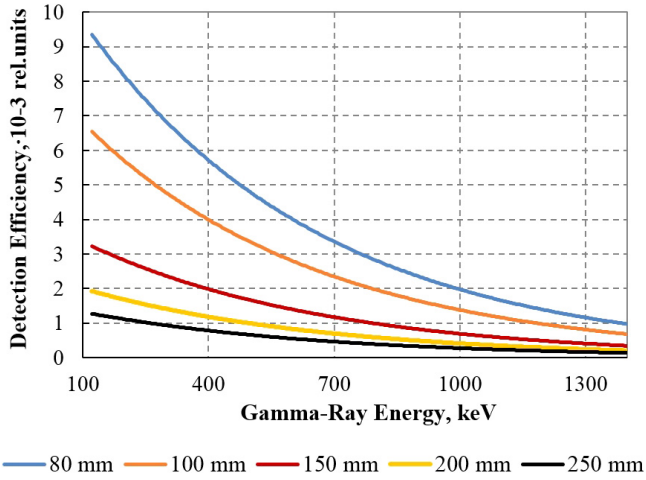

Fig. 4. (Color online) Variation of detection efficiency versus gamma ray energy for different source-to-detector distances.

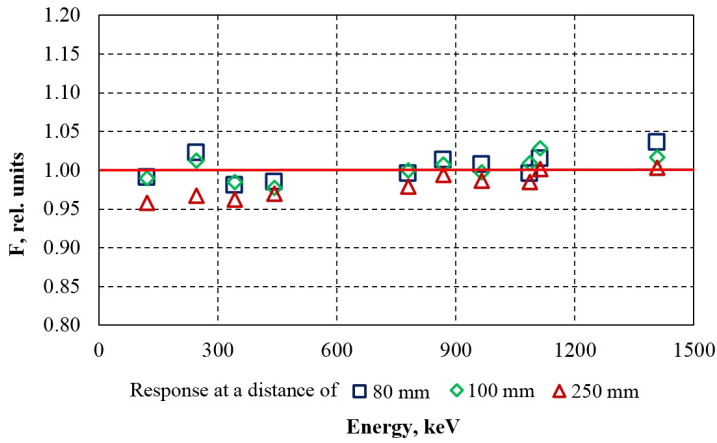

Fig. 5. (Color online) A comparison among simulated and measured responses of the model considered in this study. The measured data have been taken as true values and set as unity for a better comparison.

The studies confirm that the minimum deviations of the detection efficiency calculated with the MCNP5 and the corresponding measurement may be obtained when the source-to-detector distance is about 100 mm, which is known as the optimal distance for carrying out the measurements. The detection efficiency has the largest deviations of almost all distances for gamma-ray energy of 121.78 keV, which makes the coaxial semiconductor detectors unsuitable for the low-energy gamma-ray spectroscopy. For more accurate measurements of low-energy gamma-rays, the germanium detectors with a planar geometry are commonly used. The sensitive crystal volume for Canberra GC1518 has been 61.69 cm^3. One may conclude that the constructed model, having the identical parameters of a real germanium detector, will allow the detector response calculation with an accuracy of about 3%.

2.4. *Gamma-ray self-absorption correction factor for a fuel element of low-enriched uranium*

A practical application of the calculation model developed in this study is to determine the correction factor concerning the gamma-ray self-absorption in the sample material. To this purpose, it is necessary to perform neutron transport calculations with the model of Canberra GC1518 detector in order to obtain the correction factors for fuel elements differing in the rotation around their axes and in the fuel contents. This correction factor is necessary for the analytical expressions to calculate the ^{235}U content. A fuel element manufactured for the conversion core of the IVG.1M reactor is a spiral fuel rod of a two-bladed profile made of zirconium and a fuel core (i.e. a composition of metallic uranium and zirconium). The main physical data required for the calculation of the correction factor has been listed in Table 2.

Table 2. Physical data for gamma-ray correction factor calculations.

Parameter	Value
Gamma-ray energy, keV	185.7
Zirconium density, g/cm^3	6.51
Uranium density, g/cm^3	18.88
Source-to-Canberra GC1518 detector, mm	50
Length of sample fuel rod, mm	20

Table 3. Additional geometry-material data for gamma-ray correction factor calculation.

Uranium content in fuel core, mass.%	V(U), cm^3 (fuel core $L = 1$ cm)	V(Zr), cm^3 (fuel core $L = 1$ cm)	Density fuel core, g/cm^3	Uranium content in fuel core, mass.%
0	0	$2.22 \cdot 10^{-2}$	6.510	0.00
8	$6.67 \cdot 10^{-4}$	$2.16 \cdot 10^{-2}$	6.881	4.43
14	$1.21 \cdot 10^{-3}$	$2.10 \cdot 10^{-2}$	7.183	7.86
17	$1.49 \cdot 10^{-3}$	$2.08 \cdot 10^{-2}$	7.336	9.53
21	$1.90 \cdot 10^{-3}$	$2.04 \cdot 10^{-2}$	7.567	12.00

Some additional geometry-material data have been given in Table 3 (the obtained data for different uranium content in the fuel core) which are the volume of uranium V(U) and zirconium V(Zr) in the fuel core calculated per unit length of the fuel element, density and uranium content in the fuel core.

A number of correction factor calculations has been performed using the MCNP5 program. The calculations have been carried out for two geometries of the sample which differ in rotation around its axis by 90 degrees. To simplify the modeling, the fuel elements have been divided into a number of 2.5 mm long segments which are rotated relative to neighboring segments by 30 degrees around the axis of symmetry.

Figure 6 is an output of Visual Editor Dialog window representing two different configurations of the fuel segments. Since the gamma-ray self-absorption correction is influenced by both the geometry and the material of the source, one may conclude that the first model has the largest total absorbing area which results in maximum gamma-ray self-absorption.

The calculations have been made for 2.0E7 primaries which is sufficiently large for the desired accuracy. The correction factor K is calculated by the following formula:

$$K = \frac{\epsilon_{\text{point}}}{\epsilon_{\text{sample}}}, \tag{1}$$

where ϵ_{point} and ϵ_{sample} are the gamma-ray detection efficiencies for a nonabsorbing gamma-ray point source and a sample of a fuel element at 185.7 keV, respectively, placed on a distance of 50 mm from the detector housing.

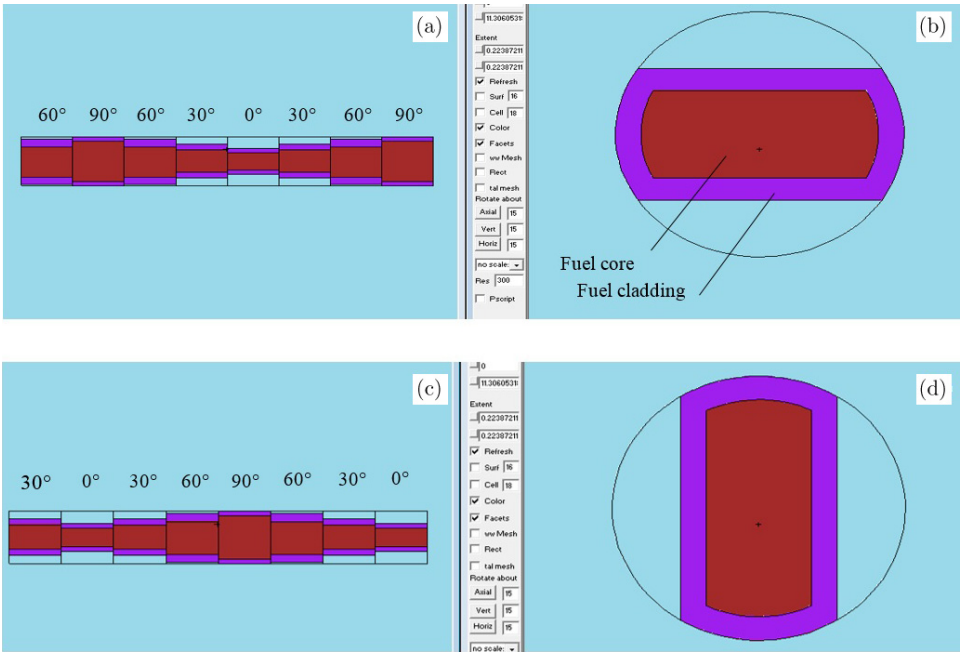

Fig. 6. (Color online) Visual Editor graphical output of two different geometrical configurations for gamma-ray self-absorption calculations. Model with maximum gamma-ray self-absorption: (a) lateral view; (b) cross-section of the central section. Model with minimum gamma-ray self-absorption: (c) lateral view; (d) cross-section of the central section.

3. Results and Discussion

The MCNP5 calculations have been performed and the 185.7 keV gamma-ray self-absorption correction factors for two different geometrical models with different uranium contents in the fuel element are listed in Table 4.

The average difference in self-absorption correction factors for the two different cases (i.e. models with maximum and minimum self-absorption) is about 0.58%

Table 4. The 185.7 keV gamma-ray correction factors calculated with the MCNP5 code.

Uranium content in fuel core, mass.%	Gamma-ray detection efficiency $\varepsilon_{\text{sampl}} \cdot 10^{-2}$, R.U.			Self-absorption correction factor K	
		Sample position with respect to the axis			
	$\varepsilon_{\text{point}} \cdot 10^{-2}$	Vertical	Horizontal	Vertical	Horizontal
0		1.79	1.78	1.145	1.151
4.43		1.73	1.72	1.189	1.196
7.86	2.053	1.67	1.66	1.226	1.233
9.53		1.65	1.64	1.245	1.253
12.00		1.61	1.60	1.272	1.280

Table 5. Comparison of correction factors for different uranium gamma-ray lines.

Uranium content in the fuel core, mass.%	143.8 keV line		185.7 keV line		205.3 keV line	
	$\varepsilon_{\text{point}} = 0.01870$		$\varepsilon_{\text{point}} = 0.02053$		$\varepsilon_{\text{point}} = 0.01863$	
	$\varepsilon_{\text{sampl}} \cdot 10^{-2}$	K	$\varepsilon_{\text{sampl}} \cdot 10^{-2}$	K	$\varepsilon_{\text{sampl}} \cdot 10^{-2}$	K
0	1.65	1.132	1.78	1.145	1.83	1.020
4.43	1.64	1.141	1.72	1.189	1.82	1.025
7.86	1.62	1.154	1.66	1.226	1.81	1.033
9.53	1.61	1.160	1.64	1.245	1.80	1.037
12.00	1.60	1.173	1.60	1.272	1.79	1.044

which increases with the uranium content of the sample. The self-absorption correction factor increases with increasing uranium content; hence, the uranium rod density which in turn increases the gamma-ray linear attenuation coefficient.

In order to obtain a more reliable result, the calculations were carried out for other two ^{235}U lines of 143.8 and 205.3 keV, in addition to 185.7 keV. The data are presented in Table 5 for the horizontal orientation of the sample.

The results can be summarized as follows. A hyper-pure germanium detector has been simulated using the MCNP5 code. It has been shown how different parameters of the detector crystal affect the detection efficiency. Since no data was available on the locations of the electrodes, two models of Canberra GC1518 detector different in the way a lithium electrode is included in the germanium detector have been proposed. The comparison proves that Model 1 has smaller deviations from the measurement and it is more appropriate for further calculations. Next, it has been determined how the dead layer thickness and the corresponding crystal volume alter the detection efficiency. Therefore, in order to calculate the effective dead layer thickness, an additional layer of germanium (i.e. the dead layer) has been added to the crystal geometry model. It is not structurally different from the base material of the crystal, but it can influence the detection efficiency. The results show that for both the top and side dead layers, the effective thickness is about 0.7 mm. Accordingly, the sensitive crystal volume for the model of Canberra GC1518 was 61.69 cm^3.

It was also found that the optimal source-to-detector distance is 100 mm at which the deviations of the calculated detection efficiencies from the corresponding measured values are minimal (the average percentage for all energies is about 1.24%). The maximum deviation for almost all distances is observed at 121.78 keV, since the coaxial detectors are poorly suited for low-energy gamma-ray spectroscopy.

Furthermore, the gamma-ray self-absorption coefficients have been calculated for complex-geometry fuel rod samples different in both the spatial orientation and uranium contents. The gamma-ray self-absorption correction factors for two different models with maximum and minimum self-absorption have been calculated which support an average 0.58% with the same uranium content despite this difference increases with the uranium content. The density of a uranium alloy rod increases as

the uranium content increases in the sample which brings out the increase in both the gamma-ray linear attenuation and self-absorption coefficients.

4. Conclusions

In this study, a computational model of an HPGe detector has been developed using the MCNP5 code. It has been shown how different parameters of the detector crystal affect the detection efficiency. An analysis has been carried out on the dependency of detection efficiency on the dead layer thickness of germanium crystal. Having developed a computation model of the crystal, a set of correction factors was extracted for the gamma-ray self-absorption within the source volume. In particular, the gamma-ray self-absorption coefficients have been calculated the fuel rod for the IVG.1M reactor which differs in both the spatial orientation and uranium contents. In this way, the simulated model of the HPGe detector of this study can be used to calculate the detection efficiency when the samples do not have a standard geometry which in turn requires self-absorption considerations. The simulated model of the HPGe detector can successfully determine the detector response with an accuracy of about 3% which is ideal in experimental studies. In such cases, a precise detector model is required for simulating different measurement setups in which the detection efficiency may alter, for instance, while performing the conversion of the IVG.1M reactor core to the low-enrichment fuel.

Acknowledgment

This research is supported by Tomsk Polytechnic University within the framework of Tomsk Polytechnic University Competitiveness Enhancement Program.

References

1. S. R. Cherry, J. A. Sorenson and M. E. Phelps, *Physics in Nuclear Medicine*, 4th edn. (Elsevier, 2012).
2. S. Tavernier, *Experimental Techniques in Nuclear and Particle Physics* (Elsevier, 2010).
3. G. F. Knoll, *Radiation Detection and Measurements*, 4th edn. (John Wiley & Sons, New York, 2010).
4. S. M. Sze and K. K. Ng, *Physics of Semiconductor Devices*, 3rd edn. (John Wiley & Sons, New York, 2006).
5. A. Tomal, J. C. Santos, P. R. Costa, A. H. Lopez Gonzales and M. E. Poletti, *Appl. Radiat. Isot.* **100**, 32 (2015).
6. E. Andreotti, M. Hult, G. Marissens, G. Lutter, A. Garfagnini, S. Hemmer and K. Von Sturm, *Appl. Radiat. Isot.* **87**, 331 (2014).
7. J. Ròdenas, A. Pascual, I. Zarza, V. Serradell, J. Ortiz and L. Ballesteros, *Nucl. Instrum. Methods Phys. A* **496**, 390 (2003).
8. A. Elanique, O. Marzocchi, D. Leone, L. Hegenbart, B. Breustedt and L. Oufni, *Appl. Radiat. Isot.* **70**, 538 (2012).
9. Yu. B. Gurov, S. V. Isakov, V. S. Karpukhin, S. V. Lapushkin, V. G. Sandukovsky and B. A. Chernyshev, *Instrum. Exp. Tech.* **51**, 59 (2008).

10. J. F. Briesmeister, *MCNP: A General Monte Carlo N-Particle Transport Code, Version 4C, LA-13709-M* (Los Alamos National Laboratory, USA, 2000).
11. M. T. Haj-Heidari, M. J. Safari, H. Afarideh and H. Rouhi, *Radiat. Meas.* **88**, 1 (2016).
12. Coaxial Germanium Detectors with Reversing Electrodes, Canberra Industries, www.canberra.com.
13. E. Tomarchio, *Radiat. Phys. Chem.* **85**, 53 (2013).
14. M. Schläger, *Nucl. Instrum. Methods A* **580**, 137 (2007).
15. N. Quang Huy, *Nucl. Instrum. Methods A* **621**, 390 (2010).